Physics of Fluids

Compressible effects modeling for turbulent cavitating flow in a small venturi channel: An empirical turbulent eddy viscosity correction

Cite as: Phys. Fluids **33**, 035148 (2021); https://doi.org/10.1063/5.0041463
Submitted: 23 December 2020 • Accepted: 15 February 2021 • Published Online: 24 March 2021

Xin-Lei Zhang (张鑫磊), Ming-Ming Ge (葛明明), Guang-Jian Zhang (张光建), et al.

Physics of Fluids ARTICLE scitation.org/journal/phf

Compressible effects modeling for turbulent cavitating flow in a small venturi channel: An empirical turbulent eddy viscosity correction

Cite as: Phys. Fluids **33**, 035148 (2021); doi: 10.1063/5.0041463
Submitted: 23 December 2020 · Accepted: 15 February 2021 ·
Published Online: 24 March 2021 · Corrected: 25 March 2021

Xin-Lei Zhang (张鑫磊),[1,2] Ming-Ming Ge (葛明明),[3] Guang-Jian Zhang (张光建),[1,3] and Olivier Coutier-Delgosha[1,3,a)]

AFFILIATIONS

[1]Univ. Lille, CNRS, ONERA, Arts et Métiers ParisTech, Centrale Lille, FRE 2017-LMFL-Laboratoire de Mécanique des fluides de Lille-Kampé de Feriet, F-59000 Lille, France
[2]The State Key Laboratory of Nonlinear Mechanics, Institute of Mechanics, Chinese Academy of Sciences, Beijing 100190, China
[3]Kevin T. Crofton Department of Aerospace and Ocean Engineering, Virginia Tech, Blacksburg, Virginia 24060, USA

[a)]Author to whom correspondence should be addressed: ocoutier@vt.edu

ABSTRACT

The Reynolds-averaged Naviers-Stokes (RANS) method coupling with cavitation model is still a practical tool to predict cavitating flows, particularly in industrial applications, due to its computational efficiency. However, the compressibility effects induced by cavitation are not well considered in conventional RANS methods, which often causes the blockage of the reentrant jet and the total steadiness of the simulated cavity. To this end, modeling of compressibility effects becomes critical to predict the characteristics of unsteady cavitating flows. An empirical eddy viscosity correction [Reboud*et al.*, "Two phase flow structure of cavitation: experiment and modeling of unsteady effects," in 3rd International Symposium on Cavitation CAV1998, Grenoble, France (1998), Vol. 26.] was proposed to consider the compressibility effects induced by cavitation. Although this modification is able to capture unsteady behaviors of cavitating flows in various configurations, it is still not fully analyzed in terms of the turbulent quantities, e.g., Reynolds shear stress. In this work, we investigate the effects of this compressibility correction on the Reynolds shear stress, by comparing with x-ray experimental data in a small Venturi channel. It is shown that the Reboud correction reduces the eddy viscosity in the entire cavity region, which improves the prediction of Reynolds shear stress near the wall significantly. However, the correction depends only on the simulated mixture density, leading to poor predictions near the phase interface where the simulated mixture density has large discrepancies. Based on the results, we propose an empirical eddy viscosity limiter to confine the original correction beneath the cavitating layer and demonstrate the merits of the proposed correction by comparing with experimental measurements.

I. INTRODUCTION

Turbulent cavitating flows commonly exist in hydraulic machineries, such as propellers, pumps, and nozzles. The occurrence of cavitation in these applications can induce various detrimental effects, including a loss of efficiency, the inception of instabilities, vibrations, noise, and erosion. In order to prevent these adverse effects, numerical simulations of cavitating flows are of critical importance for performance assessment and optimal design of the hydraulic devices.

The large eddy simulation (LES) has been increasingly introduced into numerical simulations of cavitating flows.[1–5] This method can generally provide accurate results but at considerably high computational costs. Hence, it is still not very practical to be used for flows with high Reynolds numbers in complex configurations. On the contrary, the Reynolds averaged Navier-Stokes (RANS) method can provide satisfactory predictions at much lower computational costs. For this reason, the RANS method is still the primary tool for the cavitation simulation in engineering applications. However, the RANS closure model is usually based on the assumptions of equilibrium and isotropic turbulence, and the cavitation model considers the dual-phase flow as a homogeneous mixture and neglects the slip between phases, both of which likely lead to large discrepancies of the RANS prediction for cavitating flows. Additionally, the vapor/liquid mixture region in cavitating flows can reach to supersonic regime due to the dramatic drop of sound speed. Direct numerical simulation (DNS) investigations[6] have shown that the reduction of turbulent kinetic energy occurs in the supersonic boundary layer due to the

compressibility effects. RANS model cannot capture such reduction of turbulent kinetic energy (TKE) and often overestimate the turbulent eddy viscosity, which possibly damps the development of reentrant *jet* along the surface and hinders the cavity detachment from solid walls.[7] Conclusively, it is usually essential to improve the RANS method with specific modifications for cavitating flows to account for the compressibility effects.

Different approaches have been investigated for compressibility effects modeling in cavitating flows, for instance, by reducing empirical coefficient values in the k–ω shear stress transport (SST) limiter and introducing the turbulence length scale limiter[8,9] or dilatational terms.[10] Among these methods, one extensively used approach is modifying the RANS-modeled eddy viscosity based on local mixture density. This method (hereafter referred to as Reboud correction) was initially proposed by Reboud *et al.*[11] It can reduce the RANS-modeled eddy viscosity dramatically in the cavitating region with an arbitrary function based on the local void fraction. Coutier-Delgosha *et al.*[12,13] demonstrated the necessity of considering the compressibility effects in the RANS simulation of unsteady cavitating flows and validated the Reboud compressibility correction by comparing k–ϵ re-normalization group (RNG) model and k–ω model with and without the Reboud correction. They showed that the modification could remarkably improve the numerical predictions in cloud shedding frequency, mean velocity, and void fraction. Decaix and Goncalves[8] provided the comparison of a class of RANS simulations based on the k–l transport equation model with different approaches to consider the compressibility effects, including the Reboud correction. Their results further validated that the Reboud correction can achieve a fair agreement with experimental measurements in the mean void fraction and velocity.[10] Due to its robustness and ease of implementation, this correction has been extended to different configurations, such as hydrofoils,[14] inducers,[15] and pumps.[16]

Even though in some specific cases like cloud cavitation, the RANS method with the Reboud correction can provide a fair general agreement with the experimental data,[17,18] local comparisons of the void fraction, or velocity profiles usually exhibit a large discrepancy with the available experimental measurements.[19] Moreover, the aforementioned works mainly provide the comparison investigation in mean velocity and void fraction to assess the performance of the Reboud correction. Few works validated the correction in terms of the turbulent quantities associated with Reynolds stress. That is likely due to the difficulty of optical measurement techniques for the opaque cavitating flows.[20] It is well known that the fundamental problem in the RANS method is the modeling of the Reynolds stress,[21] which introduce various hypothesis such as linear eddy viscosity assumption. Therefore, it is necessary to analyze the effects of this correction on the Reynolds stress, thereby improving the RANS method for cavitating flows.

The recent development of x-ray experiments[22–24] for cavitating flow in a small Venturi-type section provides a reliable data set of turbulent quantities, such as turbulent kinetic energy and Reynolds shear stress. These data make it possible to further validate the Reboud correction and gain insights into the cavitation/turbulence interactions.[25] The goal of the present work is to assess the Reboud correction on the turbulent quantities, e.g., turbulent kinetic energy and Reynolds shear stress, and propose an improved compressibility correction based on the experimental observation.

The rest of this paper is organized as follows. In Sec. II, the governing equations for cavitation simulation are presented. Section III gives the details of the experimental and numerical setup. Section IV shows a comparison in TKE and Reynolds shear stress between RANS simulation and experiments. Inspired by the comparison results, we propose a modified eddy viscosity correction and validate the results in Sec. V. Section VI concludes the paper.

II. GOVERNING EQUATIONS

In this work, the two phases, i.e., liquid and vapor, are assumed to be strongly coupled, and the slip in the phase interface is neglected. Based on that, the two-phase flow is governed by one group of RANS equations as

$$\begin{aligned}\rho\frac{\partial u_i}{\partial t}+\rho u_j\frac{\partial u_i}{\partial x_j}&=-\frac{\partial P}{\partial x_i}+\mu\frac{\partial^2 u_i}{\partial x_j\partial x_j}-\frac{\rho\partial\overline{u_i'u_j'}}{\partial x_j}\\ \frac{\partial\rho}{\partial t}+\frac{\partial\rho u_i}{\partial x_i}&=0.\end{aligned}\tag{1}$$

The mixture density ρ is defined as

$$\rho=(1-\beta)\rho_l+\beta\rho_v,\tag{2}$$

where ρ is the mixture density, β is the void fraction, and ρ_l and ρ_v is the density of liquid and vapor, respectively. The mixture density is obtained based on cavitation model associated with local pressure. The unknown Reynolds stress in the momentum equation is constituted by turbulence models. The turbulence model and cavitation model used in the present work will be presented in Subsections II A–II C.

A. Turbulence model

Diverse turbulence models have been proposed and validated in the past decades. Here, we apply the k–ω shear stress transport (SST) model,[26] which is one widely used model in engineering applications and also has been extensively studied for numerical simulations of cavitating flows. Due to its practicability, we aim to further evaluate this model based on our x-ray experimental data and thus gain a better understanding of the deficiency of the model. In this subsection, we give a brief introduction to this model.

The k–ω SST model combines the k–ϵ model and k–ω model. Specifically, in the sub layer of the boundary layer, the model adopts the k–ω model, while in the free shear layer away from the wall, it can transform to the k–ϵ model. The eddy viscosity is constructed as

$$\mu_t=\frac{a_1\rho k}{\max(a_1\omega,SF_2)}.\tag{3}$$

The transport equation for k and ω is formulated as

$$\frac{\partial(\rho k)}{\partial t}+\frac{\partial(\rho u_j k)}{\partial x_j}=\rho P_k-\beta^*\rho\omega k+\frac{\partial}{\partial x_j}\left[\left(\mu+\sigma_k\frac{\rho k}{\omega}\right)\frac{\partial k}{\partial x_j}\right],\tag{4a}$$

$$\frac{\partial(\rho\omega)}{\partial t}+\frac{\partial(\rho u_j\omega)}{\partial x_j}=\gamma\frac{\omega}{k}P_k-\beta\rho\omega^2+\frac{\partial}{\partial x_j}\left[(\mu+\sigma_\omega\mu_t)\frac{\partial\omega}{\partial x_j}\right],\tag{4b}$$

$$+2(1-F_1)\frac{\rho\sigma_{\omega2}}{\omega}\frac{\partial k}{\partial x_j}\frac{\partial\omega}{\partial x_j},\tag{4c}$$

where

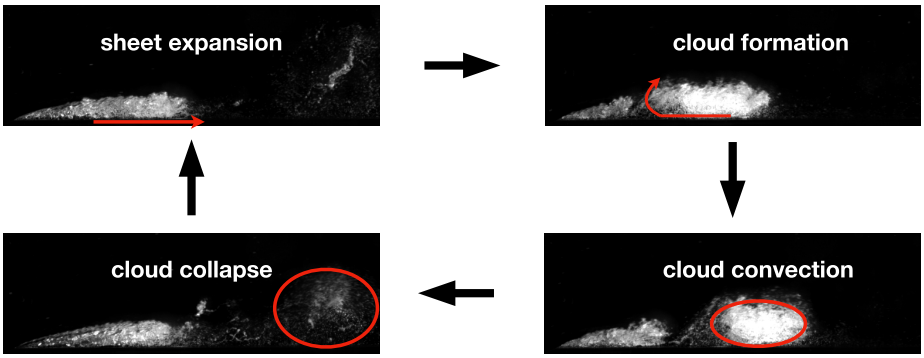

FIG. 1. A cycle of cavitation behavior.

$$F_2 = \tanh\left[\left[\max\left(\frac{2\sqrt{k}}{\beta^*\omega y}, \frac{500\nu}{y^2\omega}\right)\right]^2\right], \tag{5a}$$

$$P_k = \min\left(\tau_{ij}\frac{\partial U_i}{\partial x_j}, 10\beta^* k\omega\right). \tag{5b}$$

The limiter $10\beta^* k\omega$ for the TKE production P_k is recommended by Menter.[27] The blend function F_1 is defined as

$$F_1 = \tanh\left\{\left\{\min\left[\max\left(\frac{\sqrt{k}}{\beta^*\omega y}, \frac{500\nu}{y^2\omega}\right), \frac{4\sigma_{\omega 2}k}{CD_{k\omega}y^2}\right]\right\}^4\right\}, \tag{6}$$

where

$$CD_{kw} = \max\left(2\rho\sigma_{\omega 2}\frac{1}{\omega}\frac{\partial k}{\partial x_i}\frac{\partial \omega}{\partial x_i}, 10^{-10}\right). \tag{7}$$

The parameter in the model is blended from the k–ω model and k–ϵ as

$$\phi = \phi_1 F_1 + \phi_2(1 - F_1), \tag{8}$$

where ϕ_1 stands for the constant with subscript 1, while ϕ_2 is the constant with subscript 2. The constants in the model are given as

$$\gamma_1 = \frac{5}{9}; \quad \gamma_2 = 0.44; \quad \alpha_1 = \frac{5}{9}; \quad \alpha_2 = 0.44; \quad \beta_1 = \frac{3}{40};$$
$$\beta_2 = 0.0828; \quad \beta^* = \frac{9}{100}; \quad \sigma_{k1} = 0.85; \quad \sigma_{k2} = 1; \quad \sigma_{\omega 1} = 0.5;$$
$$\sigma_{\omega 2} = 0.856. \tag{9}$$

B. Modeling of compressibility effects

Cavitating flows are usually highly unstable with fluctuations at various scales. The unsteady cavitation typically has periodic behaviors with four different stages in each cycle, as shown in Fig. 1. The cavitation first expands along the wall and forms the cloud cavitation. Then the cavity detaches from the wall and is driven by the main stream to the wake, eventually breaking up in the zone of high pressure.

Cloud cavitation is characterized by a primary large scale instability based on the periodic shedding of the rear part of the cavity. However, the conventional RANS models cannot capture the shedding behavior, because the eddy viscosity in the cavitation region is overestimated and thus blocks the reentrant jet, which is the main factor to induce the bubble separation. In order to capture the shedding behavior, Reboud *et al.*[11] imposed an artificial modification $f(\rho)$ on the original eddy viscosity as a multiplicative correction. The modification reduces the eddy viscosity dramatically in the cavitation regime based on the extent of vaporization. The formulation can be expressed as

$$f(\rho) = \rho_v + (1 - \beta)^n(\rho_l - \rho_v). \tag{10}$$

The plot of $f(\rho)$ is shown in Fig. 2. When the void fraction is equal to zero, $f(\rho)$ equals the liquid density as in the original model. Conversely, when the void fraction decreases to 1, $f(\rho)$ will be the vapor density. For intermediate values of void fraction, the function significantly reduces the RANS-modeled eddy viscosity once there occurs the cavitation. Different investigations have been carried out and demonstrated the success of this modification to simulate unsteady cavitating flows in different geometries.[7,14,28] With this modification, the periodic behavior can be correctly reproduced, usually with the shedding frequency in fair agreement with experimental observations.

C. Phase model

Regarding the phase model, here we apply the barotropic state law due to its robustness. Specifically, for the pure liquid and vapor,

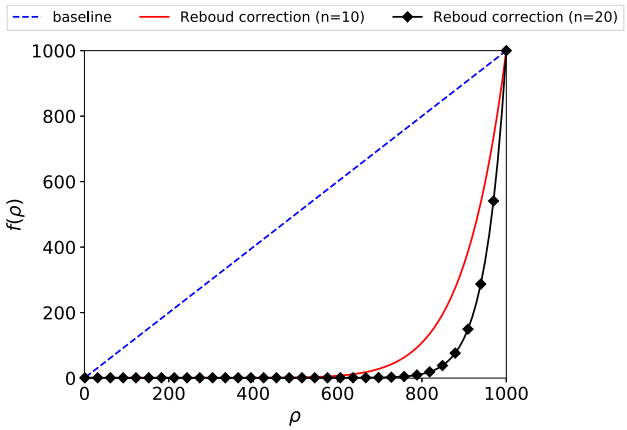

FIG. 2. Plot of the Reboud correction function $f(\rho)$.

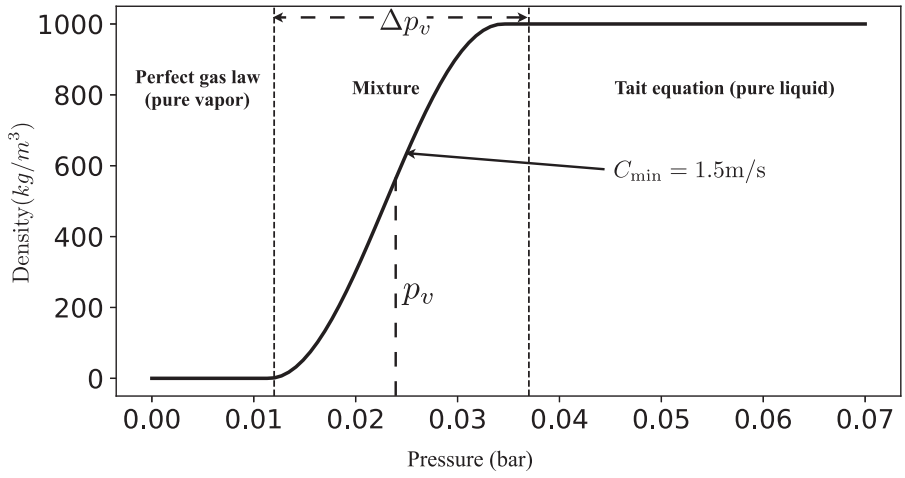

FIG. 3. Plot of the barotropic state law for the mixture.

the Tait equation and the perfect gas law are utilized to estimate the relationship between the pressure and the density. The formulations are shown as

$$\frac{\rho_l}{\rho_{\text{ref}}} = \sqrt[7]{\frac{P + P_0}{P^T_{\text{ref}} + P_0}}, \qquad \frac{P}{\rho_v} = C, \tag{11}$$

where P^T_{ref} and ρ_{ref} is the reference pressure and density, $P_0 = 3 \times 10^8$ Pa. In the mixture interval, the state law is characterized with a sinusoidal transition. The maximum slope is defined by $1/C^2_{\min}$, where $C_{\min} = \partial P/\partial \rho$. The plots are shown in Fig. 3 with $C_{\min} = 1.5$ m/s. The value of $C_{\min}$ is determined based on our previous investigation.[7] It is noted that the sound speed with the present density definition, i.e., Eq. (2), would incur enormous errors in the computation of sound speed.[29] The correct density definition was proposed by Singhal *et al.*[30] and has been shown to better estimate the flow pulsations.[29] It would be interesting to employ the correct density definition to improve the CFD predictions. But it is not the focus of the present work, and further analysis in terms of sound speed estimation is worthy of future studies.

III. TEST CASE

A. Simulation setup

Fast x-ray imaging experiments were conducted in Argonne National Laboratory to obtain a set of reliable data for cavitating flows, including turbulent kinetic energy and Reynolds shear stress. We use the x-ray data to validate and improve the current RANS method. For details about the experimental apparatus, readers are referred to Refs. 22 and 24 The Venturi-type channel used in this work is shown in Fig. 4, which has an 18° convergent angle and an 8° divergent angle. The inlet section is a rectangular with 17 mm × 4 mm. To keep consistency with the experimental condition, the inlet velocity is calculated to be 8.6 m/s, the cavitation number based on the outlet pressure is 1.15, and the Reynolds number is 1.9×10^5. The profiles with the index from 1 to 4

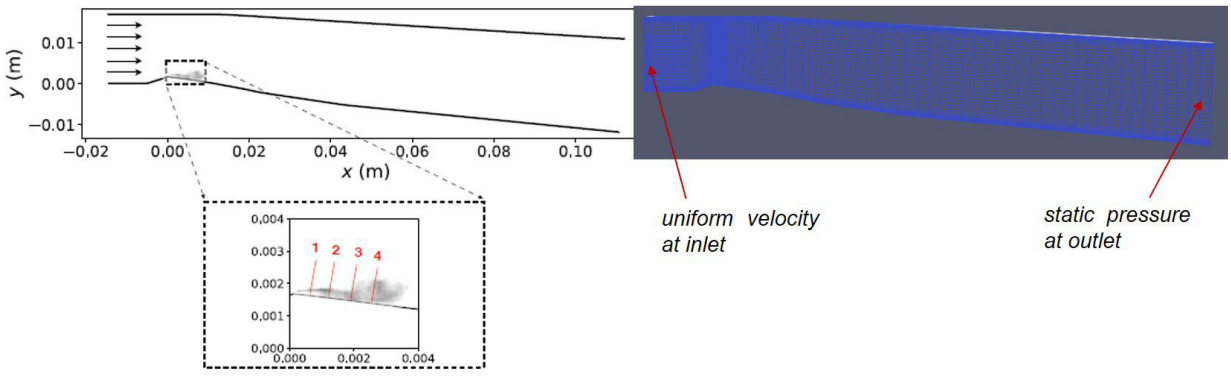

FIG. 4. Schematic of the computational domain. The profiles with index of 1 to 4 in the zoom window, indicating $x = 0.0003, 0.0008, 0.0018, 0.0025$ m, are used for comparison in the following sections.

TABLE I. Convergence study of time step and mesh grid.

Time step (T/T_{ref})	Mesh	Cavity length	Shedding frequency
0.005	160 × 50	13.4 mm	222 Hz
0.005	270 × 117	11.0 mm	230 Hz
0.005	400 × 200	10.8 mm	232 Hz
0.001	270 × 117	10.8 mm	230 Hz
0.005	270 × 117	11.0 mm	230 Hz
0.01	270 × 117	12.3 mm	222 Hz

TABLE II. Summary of simulation results with k–ω SST turbulence model with comparison to the experiments.

Case	Cavitation number	Cavity length	Shedding frequency
k–ω SST	1.12	11.0 mm	230 Hz
Exp	1.15	10 ± 1.0 mm	210 ± 20 Hz

in the zoomed window, indicating $x = 0.0003$, 0.0008, 0.0018, 0.0025 m, are used for comparison in Secs. IV and V B. The mesh in the computational domain is constituted with 260 cells in the streamwise direction and 117 cells in the normal to wall direction. The time step is 0.005 of the reference time. The convergence study of the time step and mesh grid is shown in Table I. The reference length L_{ref} is 0.0224 m, and the reference velocity U_{ref} is 8.6 m/s. The cavitation number for the simulation is given as 1.12 to have a similar cavity length and shedding frequency compared to the experiment. Uniform velocity is imposed at the inlet of the computational domain, and static pressure is imposed at the outlet. The wall function is applied along the solid wall, and the y plus in the first mesh adjacent to the wall ranges from 15 to 20. Based on previous works,[10,13] the y plus is adequate to simulate cavitation in such a Venturi-type section. The 2D RANS equation coupling with barotropic state law is solved to predict the cavitating flow.

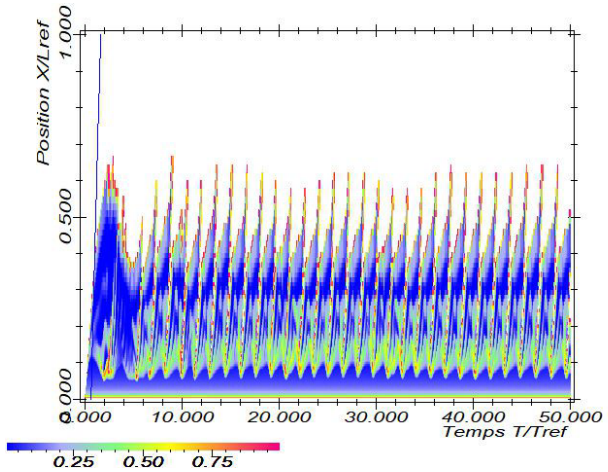

FIG. 5. Time evolution of cavity shape from the k–ω SST simulation.

B. Numerical methods

The numerical simulations are conducted in a home-made two-dimensional CFD code, which has been developed and validated over decades.[7,17,31] In the code, the second-order implicit scheme is used for temporal discretization, and the finite volume method is applied for the spatial discretization. The second-order scheme will locally switch to the first order in the region existing a large pressure gradient to prevent numerical oscillations. The oscillation-free second-order HLPA scheme[32] is leveraged to estimate the convection term, and the central difference scheme is adopted for the diffusion term. The SIMPLE algorithm[33] is used to solve the coupling of pressure and velocity.

IV. NUMERICAL RESULTS

In this section, we compare the turbulent quantities between the RANS simulation and the experiment. The results are summarized in Table II. The plot of the time evolution of cavity shape from RANS

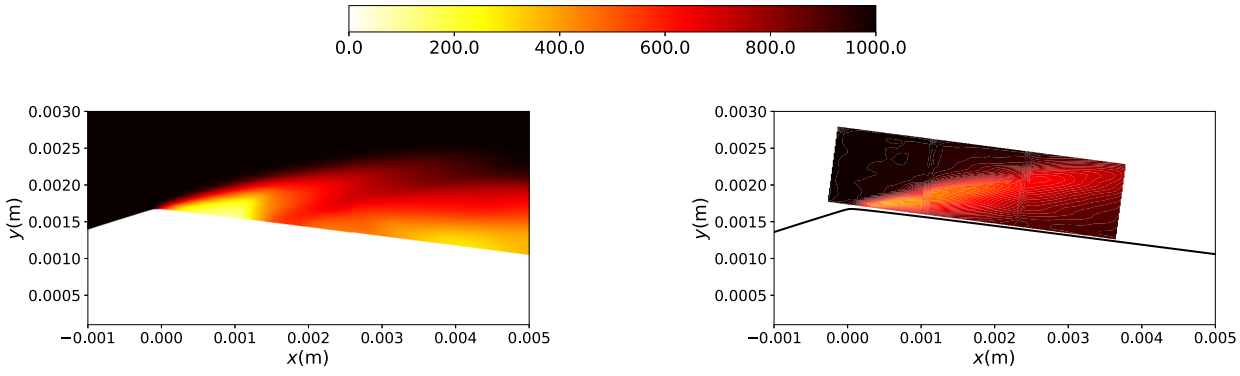

(a) k–ω SST (b) experiment

FIG. 6. Contour plots of time-averaged cavity shape from (a) the RANS simulation with k–ω SST model and (b) the experiments.

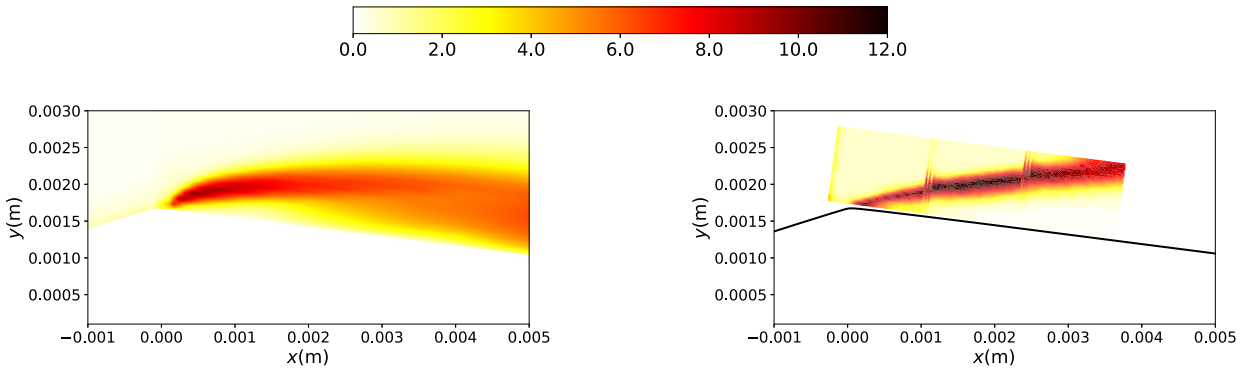

(a) k–ω SST (b) experiment

FIG. 7. Contour plots of time-averaged turbulent kinetic energy from (a) the RANS simulation with k–ω SST model and (b) the experiments.

simulations is presented in Fig. 5, indicating the shedding frequency and the mean cavity length. With the k–ω SST turbulence model, a small sheet cavity with 0.001 m length near the throat can be observed, and the cavity is expanded from that.

Figure 6 represents the comparison between the numerical simulation and the experiment in the mixture density. It can be seen that the shape of the cavity is not well predicted. First, the position of the detached cavity is very upstream relative to the numerical simulation.

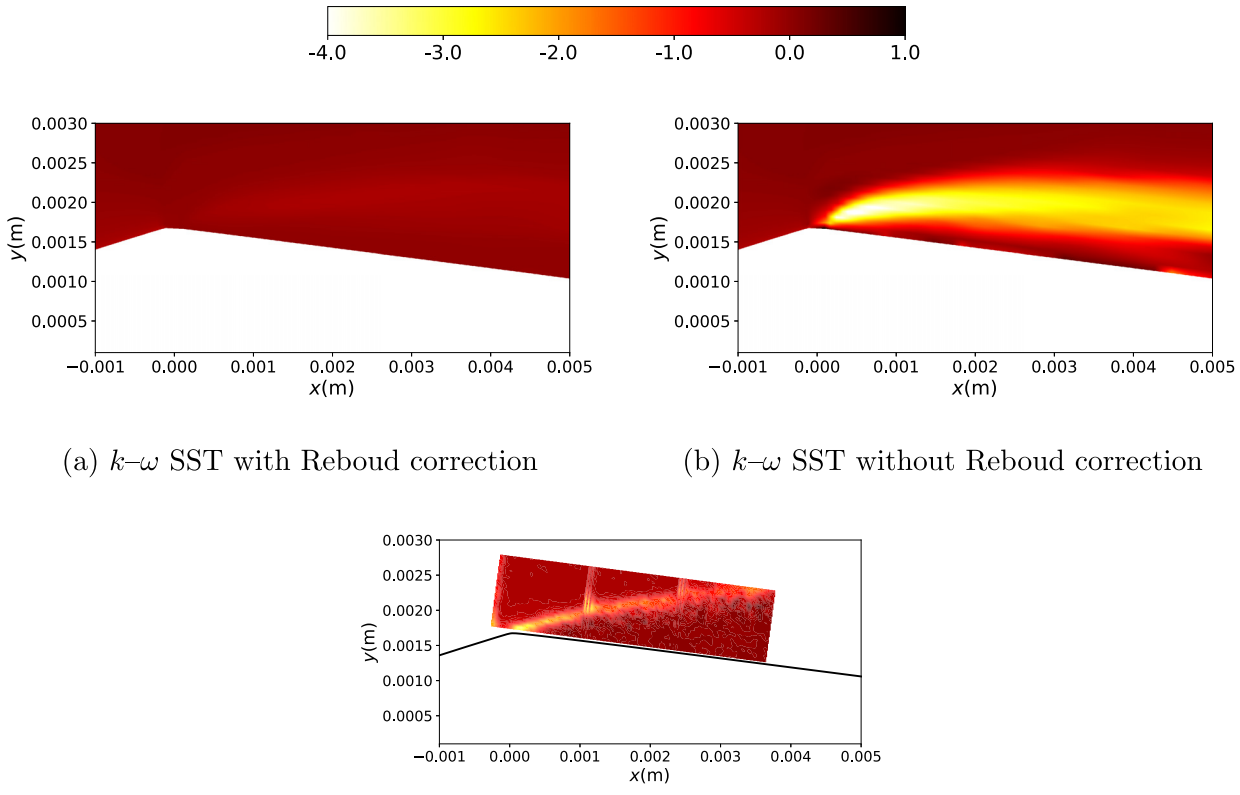

(a) k–ω SST with Reboud correction (b) k–ω SST without Reboud correction

(c) experiment

FIG. 8. Contour plots of time-averaged Reynolds shear stress from (a) RANS simulations with Reboud correction, (b) RANS simulations without Reboud correction, and (c) the experimental measurements.

On the other hand, the lowest density in the simulation reaches below 300 kg/m^3, while the minimum density from experimental observation is around 600 kg/m^3. The separated cavity in the numerical prediction is reattached in the downstream and the total attached part is longer than the experimental measurements. The comparison results of the density as well as the velocity along profiles are presented in Fig. 9. It clearly shows that the results in both density and velocity exhibit large discrepancies with k-ω SST model.

The contour plots of turbulent kinetic energy with comparison to experiments are presented in Fig. 7. From the results, it can be seen that the k–ω SST model can capture the high turbulent kinetic energy areas. However, at the downstream, the value is overestimated near the wall. Further, we provide the comparison along profiles as shown in Fig. 7. At the first position, the predicted turbulent kinetic energy matches well with the experiments. As for the downstream where the cavity detachment occurs in the experiment, the TKE reduces to around zero in the region near the wall. However, the TKE from numerical simulations decreases slowly along the wall and remains turbulent fluctuations near the wall at position 3 and 4, which leads to a large discrepancy between the numerical simulation and experiments. We also compare the solved turbulent kinetic energy, and the results show that in the upstream mainly the modeled TKE is dominant. Hence we only provide the comparison between the modeled TKE and experimental data, and the results of the solved TKE are omitted for brevity.

The contour plots of numerical results and the experimental data in Reynolds shear stress are shown in Figs. 8(a) and 8(c), respectively. It is noticeable that the $k-\omega$ SST model with Reboud correction provides a very low Reynolds shear stress compared to the experiments. In order to investigate the effects of the Reboud correction on the Reynolds shear stress, we also perform the simulation without Reboud correction. The contour plot of the results is shown in Fig. 8(b). It can be seen that without Reboud correction, the k–ω SST model can capture the region where high Reynolds shear stress exists but overestimates the Reynolds stress near the wall. Figure 9(d) presents the comparison results in the Reynolds shear stress along profiles. At the first position, a good agreement with experiments can be observed without Reboud correction. While approaching the downstream, there will be a large discrepancy near the wall. That may be due to the discrepancy in TKE, as shown in Fig. 9(c). With Reboud correction, we can have a good estimation in Reynolds shear stress near the wall. In contrast, in the region away from the wall, the correction worsens the prediction and exhibits a large discrepancy from the experiments.

The numerical results show that the $k-\omega$ SST model cannot simulate well the Reynolds shear stress in the near-wall region if Reboud correction is not employed. The large discrepancy can be explained from several aspects. First, the slip between phases probably causes the observed high TKE, but the conventional RANS models do not consider this specific effect. Besides, the TKE at the upstream can be well estimated based on the comparison, and hence it is possible to predict well the Reynolds shear stress without Reboud correction. However, at the downstream, the significant reduction of TKE is not captured by the conventional RANS method without Reboud correction. This leads to large Reynolds shear stress and requests auxiliary modifications such as Reboud correction. On the other hand, the Reboud correction will significantly underestimate the Reynolds shear stress near the phase interface. That is because that the cavity shape is not accurately predicted in this case. Specifically, the global value of the mixture density near the wall from experiments is much higher than the numerical prediction. As such, depending on only the mixture density may lead to an inappropriate correction. It has been noted that the cavitation not only affects the mixture density

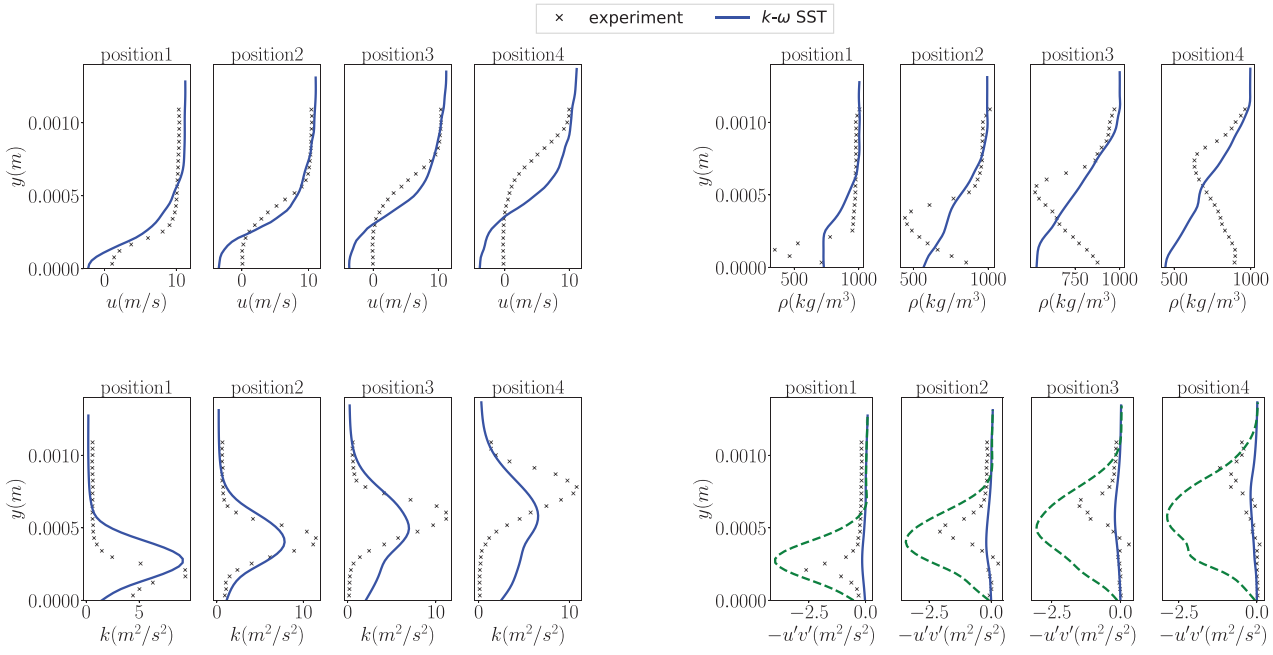

FIG. 9. Comparison in (a) velocity, (b) void fraction, (c) TKE, and (d) Reynolds shear stress between the experiments and RANS simulations. Note that the green/dashed lines in (d) indicate the results without the Reboud correction.

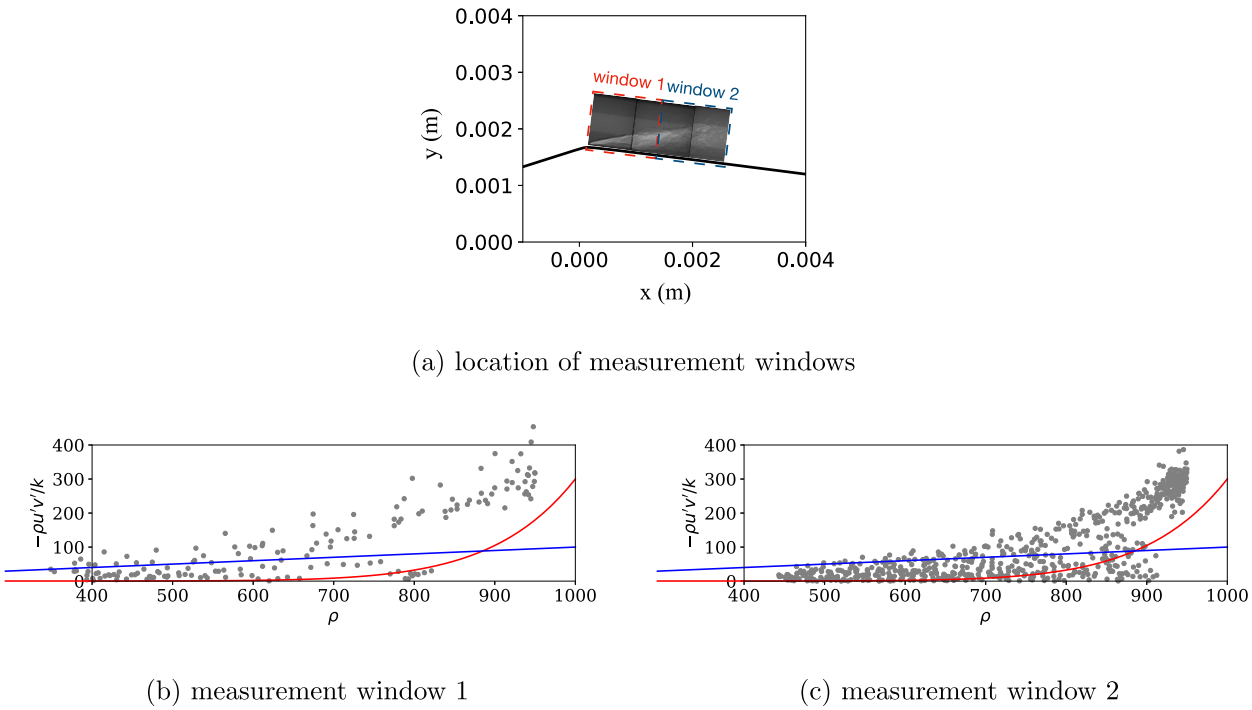

(a) location of measurement windows

(b) measurement window 1

(c) measurement window 2

FIG. 10. Comparison of the Reboud correction with $n = 10$ (red line), the Bradshaw assumption with $c = 0.1$ (blue line), and experimental data (gray dots). (a) The location of two measured windows for comparison. (b) Comparison results in the measurement window 1. (c) Comparison results in the measurement window 2.

but also can enlarge the boundary layer thickness.[34] Thus, a better modification is possible to be achieved by limiting the correction within the boundary layer, instead of only depending on the simulated mixture density. In Sec. V, we propose a modified eddy viscosity correction based on the boundary layer thickness and validate it in the numerical experiments.

V. MODIFIED EDDY VISCOSITY CORRECTION FROM EXPERIMENTAL MEASUREMENTS

In $k-\omega$ shear stress transport model, the eddy viscosity in the boundary layer is modified based on the Bradshaw assumption. That is, the ratio of Reynolds shear stress to TKE is constant as

$$\frac{-u'v'}{k} = c, \tag{12}$$

where c is constant as 0.31 for the incompressible turbulent flows. However, this ratio c is set for non-cavitating flows, while for the turbulent cavitating flow, the ratio has to be reduced based on the experimental observation.[35] The reduced constant c has been investigated to improve the accuracy of cavitation simulation.[8] It was demonstrated that with the reduced Bradshaw ratio, e.g., $c = 0.1$, the periodic cavity shedding could also be captured. In the following, we compare the ratio of the Reynolds shear stress to the TKE from experiments, in contrast to the Bradshaw assumption ($c = 0.1$) and the Reboud correction, and further modify the Reboud's eddy viscosity correction to achieve better alignment with experiments.

TABLE III. Summary of slope of cavitating mixing layer for four different flow conditions with comparison of experimental data and results of fitting formula.

Case index	Reynolds number	Cavitation number	Slope (exp)	Slope (formula)
1	1.9×10^5	1.15	0.42	0.40
2	1.9×10^5	1.25	0.36	0.36
3	2.6×10^5	1.15	0.39	0.37
4	3.0×10^5	1.15	0.38	0.36

A. Modified eddy viscosity correction

From the numerical results in Sec. IV, the Reboud correction can reduce the eddy viscosity near the wall and alleviate the blockage of the reentrant jet, thereby leading to the cloud shedding. However, in the region away from the wall, the correction worsens the predictions in Reynolds shear stress. That is likely due to that the correction only depends on the simulated mixture density, while the void fraction is usually not predicted well with existing phase models and RANS models. Here, we compute the ratio of the Reynolds shear stress and TKE based on the Reboud correction [i.e., $c \times f(\rho)$] in comparison with experimental data, as presented in Fig. 10. It is obvious that the Reboud correction can be relatively better than the Bradshaw assumption but still have a large discrepancy with experimental measurements. Moreover, the Bradshaw assumption is deduced in the boundary layer, while the Reboud correction does not consider the effects of cavitation on the boundary layer. It has been noted that the cavitation will enlarge the boundary layer.[35] Accordingly, we analyze four experimental

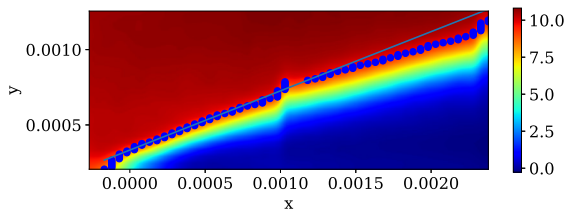

(a) $Re = 1.9 \times 10^5$, $\sigma = 1.15$

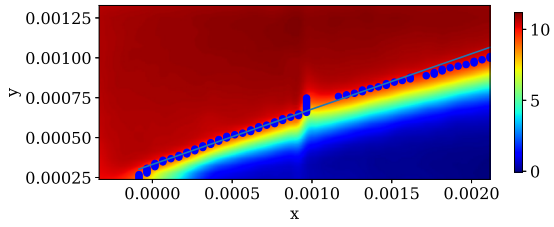

(b) $Re = 1.9 \times 10^5$, $\sigma = 1.25$

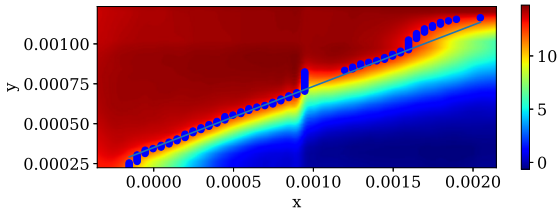

(c) $Re = 2.6 \times 10^5$, $\sigma = 1.15$

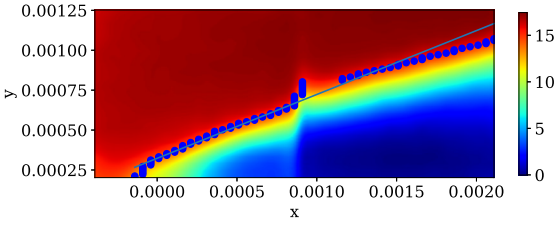

(d) $Re = 3.0 \times 10^5$, $\sigma = 1.15$

FIG. 11. Fitting slopes of the cavitating mixing layer in velocity U for experimental data with different Reynolds number (Re) and caviation number (σ). (a) $Re = 1.9 \times 10^5$, $\sigma = 1.15$, (b) $Re = 1.9 \times 10^5$, $\sigma = 1.25$, (c) $Re = 2.6 \times 10^5$, $\sigma = 1.15$, (d) $Re = 2.6 \times 10^5$, $\sigma = 1.15$.

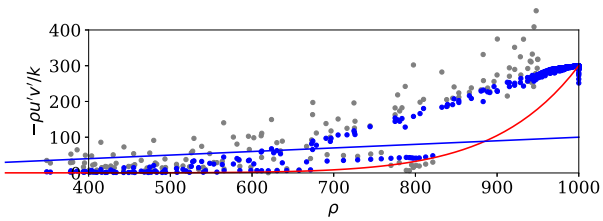

(a) $Re = 1.9 \times 10^5$, $\sigma = 1.15$

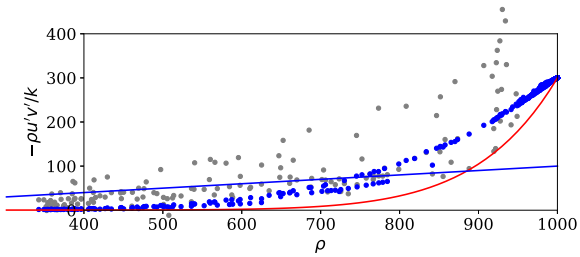

(b) $Re = 1.9 \times 10^5$, $\sigma = 1.25$

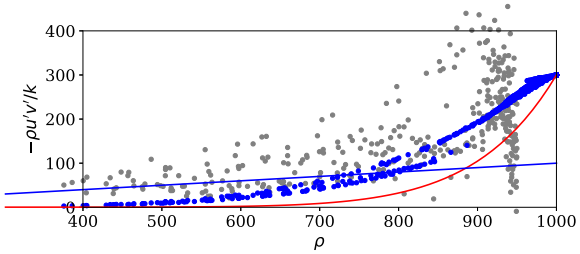

(c) $Re = 2.6 \times 10^5$, $\sigma = 1.15$

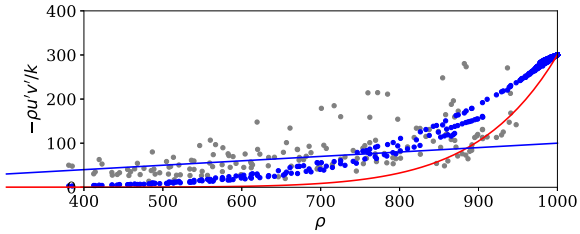

(d) $Re = 3.0 \times 10^5$, $\sigma = 1.15$

FIG. 12. Comparisons in the ratio of Reynolds shear stress and TKE within the measurement window 1. (a) $Re = 1.9 \times 10^5$, $\sigma = 1.15$, (b) $Re = 1.9 \times 10^5$, $\sigma = 1.25$, (c) $Re = 2.6 \times 10^5$, $\sigma = 1.15$, (d) $Re = 2.6 \times 10^5$, $\sigma = 1.15$. Red line: the Reboud correction with $n = 10$; blue line: the Bradshaw assumption with $c = 0.1$; gray dots: experimental data; blue dots: modified Reboud correction.

measurements with different flow conditions as shown in Table III. Herein three cases have the same cavitation number but different Reynolds numbers, and two cases have the same Reynolds number but different cavitation numbers. We estimate the thickness of cavitating mixing layer based on $u = 0.9u_{max}$ and fit the slope as shown in Fig. 11. The slope values for each case are summarized in Table III.

Based on the experimental data, we adopt the linear regression with logarithmic transformation[36] to obtain a boundary layer thickness formula for this case. The fitting formula is written as

$$\delta = \frac{5.2}{\sigma Re^{1/5}} \Delta x_i, \tag{13}$$

where Δx_i is the distance to the cavitation inception point (i.e., the throat of the Venturi channel). It is shown in Table III that the formulated boundary layer thickness can have a good agreement with experiments. Moreover, the formulation has a similar scaling exponent on the Reynolds number as the thickness formulation for turbulent boundary layer over a flat plate, i.e., $\delta = 0.37\frac{x}{Re^{1/5}}$, where x is the distance downstream from the start of the boundary layer.[37] Additionally, the cavitation number is introduced based on the experimental observation to account for the effects of cavitation on the boundary layer thickness. Based on this boundary layer estimation, we propose a modified model to trigger the eddy viscosity reduction only within the estimated boundary layer. Specifically, the dimensionless parameter n in the Reboud correction is modified to be N as

$$N = \frac{n-1}{2}\tanh\frac{\delta - y}{l_t} + \frac{n+1}{2}, \tag{14}$$

where n is the original parameter in the Reboud correction and l_c is the transition length where the parameter N transits from 1 to n gradually to ensure numerical stability. In this case, the area of 0.001m away from the throat is almost a stabilized cavity without large fluctuations as shown in Fig. 5, and hence we choose $l_c = 0.001$ m in this case, and y is the distance to the wall. With this formula, when the distance to the wall y is less than the estimated boundary layer thickness δ, N will be equal to the original n. Conversely, N will be 1 outside the estimated boundary layer region and make the correction inactive. Admittedly, the empirical parameters in the formulation of boundary layer thickness are determined based on the limited experimental data and need further validations. Nevertheless, it is noted that x-ray data of the void fraction and velocity within the vapor cavity are very difficult to be obtained due to the opacity of the cavitating bubbles. Hence, the provided estimation of the boundary layer thickness may be specific for the cavitating flow in the investigated small Venturi channel. The feasibility of the proposed method for the other configurations such as hydrofoil needs further investigation but out of the scope of the present work.

B. Validation of proposed correction

To validate the proposed correction, we first compare the proposed modification with experimental data as well as the original Reboud correction and Bradshaw assumption. The results of two different measurement windows are shown in Figs. 12 and 13, respectively. It is noticeable that the proposed modification has a better agreement with measurements than the original Reboud correction.

To further validate the modification, we apply the modified eddy viscosity correction into the four numerical test cases in Table III. The simulation results in the Reynolds shear stress are presented in Fig. 14. It can be seen that for all the cases the results can fit well with experimental data in the Reynolds shear stress $-\overline{u'v'}$, in contrast to that with

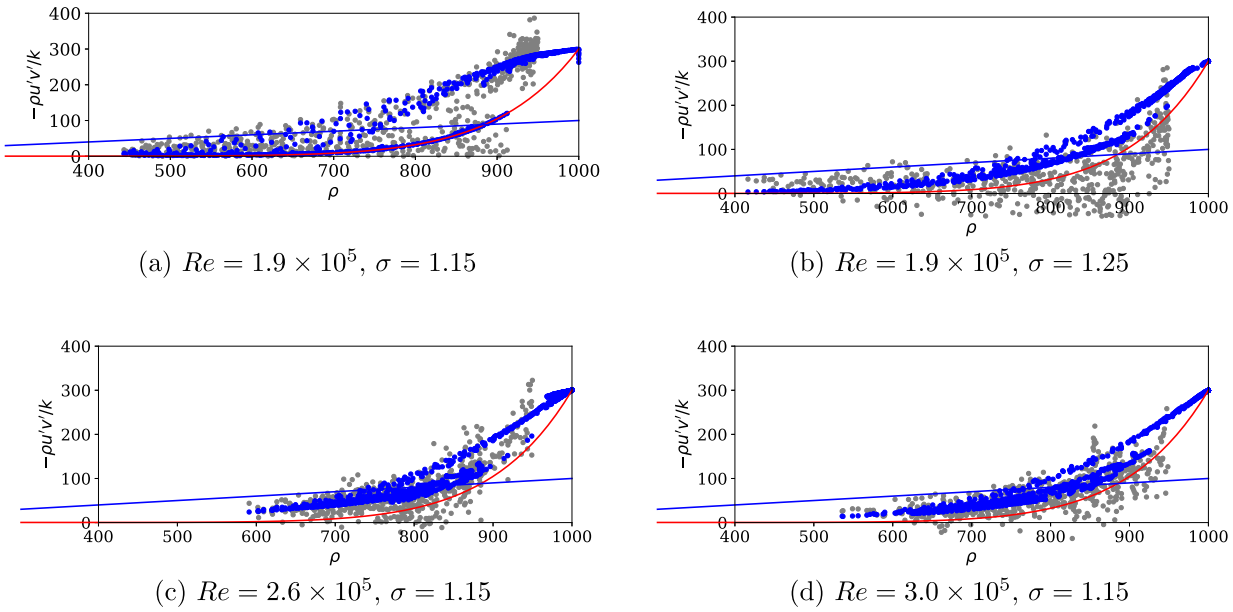

FIG. 13. Comparisons in the ratio of Reynolds shear stress and TKE within the measurement window 2. (a) $Re = 1.9 \times 10^5$, $\sigma = 1.15$, (b) $Re = 1.9 \times 10^5$, $\sigma = 1.25$, (c) $Re = 2.6 \times 10^5$, $\sigma = 1.15$, (d) $Re = 2.6 \times 10^5$, $\sigma = 1.15$. Red line: the Reboud correction with $n = 10$; blue line: the Bradshaw assumption with $c = 0.1$; gray dots: experimental data; blue dots: modified Reboud correction.

original Reboud correction. It can be demonstrated that the proposed modification is able to improve significantly the prediction in Reynolds shear stress by activating the Reboud correction within the estimated boundary layer.

Although the Reynolds shear stress can be captured with the modified eddy viscosity correction, the resolved velocity and mixture density are not improved. We take the case 1 as an example for brevity. The results of velocity and void fraction are presented in Fig. 15. It can be seen that a large discrepancy still exists between the simulation with modified Reboud correction and the experiment. This may be due to several reasons. First, this work is based on 2D simulations, but cavitating flow, especially cloud cavitation, is a typical 3D phenomenon. It was shown that the 3D simulation with the LES model and the similar homogeneous model could perform remarkably well for cloud cavitation,[5,38] and the 3D simulation may be essential to capture the cavitation–vortex interaction[4] and provides the accurate shape of shedding cavitation.[39] Also, the used cavitation model and the mixture density definition may not be sufficiently accurate to model the phase changes, which probably results in the underestimation of density near the wall. Specifically, in the experiment, the cavity in the downstream (i.e., position 3 and position 4) is detached from the wall, and the liquid occupies the regime beneath the cavitating shear layer, while it is not captured in the simulation. Moreover, the RANS equation is coupled with the cavitation model in terms of the mixture density. In the RANS equation, the low mixture density near the wall may overestimate the effects of the local adverse pressure gradient. The discrepancy in pressure gradient term could be dominant, leading to the improvement in Reynolds shear stress negligible. Additionally, it would be due to the linear turbulence model, and some nonlinear turbulence models, such as the Reynolds stress model, were observed to provide more accurate predictions.[40,41] At last, it has been demonstrated that the RANS equations are ill-conditioned.[42] That is, small errors in the Reynolds stress can result in a large discrepancy in the velocity, particularly for flows with high Reynolds numbers. Hence, the large discrepancy in velocity is not surprising, even though the Reynolds shear stress is significantly improved. Conclusively, the merits of the proposed method are demonstrated in capturing the Reynolds shear stress by comparing with our X-ray experimental data. The limitation of the method mainly lies in the limited experimental data and incapability of improving predictions of velocity and void fraction, which need extensive validations in other configurations and further improvements in the turbulence/cavitation modeling. On the other hand, this work shows that Reboud's eddy viscosity correction is able to be further improved by combining the physical knowledge (i.e., effects of the cavitation on the boundary layer

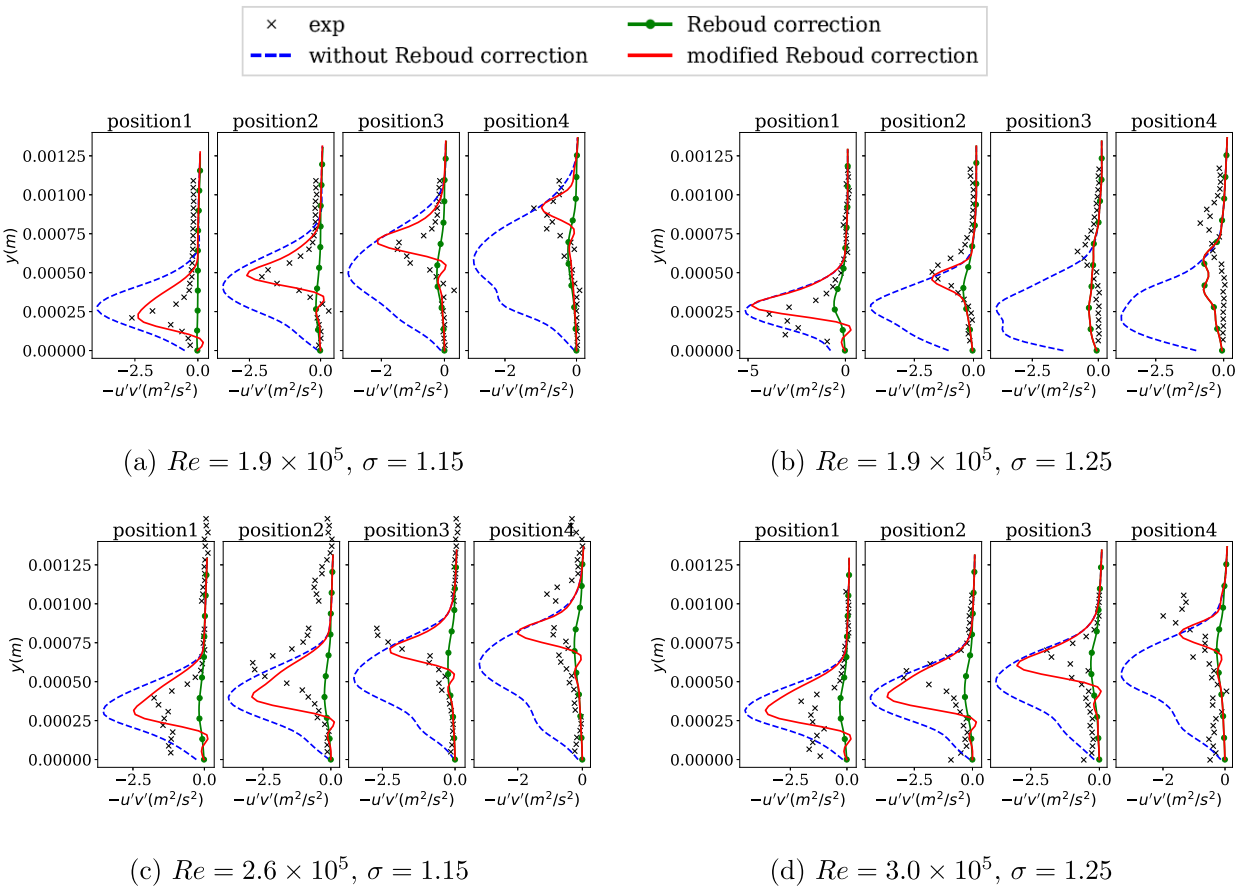

(a) $Re = 1.9 \times 10^5$, $\sigma = 1.15$

(b) $Re = 1.9 \times 10^5$, $\sigma = 1.25$

(c) $Re = 2.6 \times 10^5$, $\sigma = 1.15$

(d) $Re = 3.0 \times 10^5$, $\sigma = 1.25$

FIG. 14. Numerical comparison of the modified Reboud correction with experiment and original Reboud corrections in Reynolds shear stress. (a) $Re = 1.9 \times 10^5$, $\sigma = 1.15$, (b) $Re = 1.9 \times 10^5$, $\sigma = 1.25$, (c) $Re = 2.6 \times 10^5$, $\sigma = 1.15$, (d) $Re = 2.6 \times 10^5$, $\sigma = 1.15$.

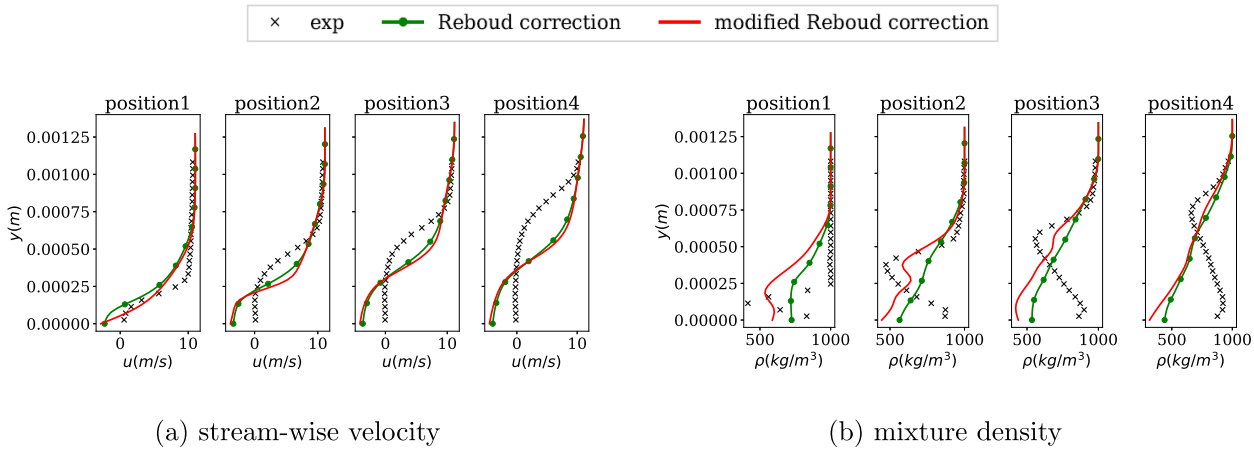

(a) stream-wise velocity (b) mixture density

FIG. 15. Comparison in (a) stream-wise velocity and (b) mixture density between modified Reboud correction and original Reboud correction.

herein) and the experimental observations. This would motivate the applications of physics-aware data-driven methods[43] in future studies of cavitation simulations.

VI. CONCLUSION

In this work, we investigate numerically the compressibility effects of cavitation on the turbulent quantities, i.e., turbulent kinetic energy and Reynolds shear stress, in a small Venturi channel. It is observed that the Reboud correction can take into account the compressibility induced by cavitation and improve the simulation results of Reynolds shear stress near the wall by comparing to the x-ray experimental data. Nevertheless, near the phase interface the results with Reboud correction exhibit very large discrepancies. This may be due to that the prediction of cavity shape is inaccurate, while the Reboud correction reduces the eddy viscosity dramatically only depending on the local mixture density. To this end, we propose an empirical estimation of the boundary layer thickness in cavitating flows and activate the Reboud correction only within the estimated boundary layer. The experimental data and numerical tests show that this modified correction can predict the Reynolds shear stress in better agreement with the experiment in contrast to the original Reboud correction.

However, the velocity and density with the modified eddy viscosity model are not improved noticeably, probably due to the 3D effects, the inadequate phase change model and turbulence model, or ill-conditioning of RANS equations. Further validations will be conducted for different cavitation/turbulence models and configurations. Additionally, this work improves the RANS prediction of cavitating flows based on the linear regression analysis, and it is appealing to introduce data-driven approaches, such as data assimilation[44] and machine learning[43,45] to build functional models for cavitation simulations based on experimental measurements or LES results.

ACKNOWLEDGMENTS

The authors would like to thank the reviewers for their constructive and valuable comments, which helped us to improve the quality and clarity of this manuscript. Part of this work has been performed under contract N00014-19-1-2019 with ONR. The authors wish to thank Dr. Ki-Han Kim for his continuous support. The use of the Advanced Photon Source at Argonne National Laboratory was supported by the U. S. Department of Energy, Office of Science, and Office of Basic Energy Sciences.

DATA AVAILABILITY

The data that support the findings of this study are available from the corresponding author upon reasonable request.

REFERENCES

[1]N. Dittakavi, A. Chunekar, and S. Frankel, "Large eddy simulation of turbulent-cavitation interactions in a Venturi nozzle," J. Fluids Eng. **132**, 121301 (2010).
[2]B. Ji, X.-W. Luo, X.-X. Peng, and Y.-L. Wu, "Three-dimensional large eddy simulation and vorticity analysis of unsteady cavitating flow around a twisted hydrofoil," J. Hydrodynamics **25**, 510–519 (2013).
[3]B. Huang, Y. Zhao, and G. Wang, "Large eddy simulation of turbulent vortex-cavitation interactions in transient sheet/cloud cavitating flows," Comput. Fluids **92**, 113–124 (2014).
[4]B. Ji, X. Luo, R. E. Arndt, X. Peng, and Y. Wu, "Large eddy simulation and theoretical investigations of the transient cavitating vortical flow structure around a NACA66 hydrofoil," Int. J. Multiphase Flow **68**, 121–134 (2015).
[5]A. Gnanaskandan and K. Mahesh, "A numerical method to simulate turbulent cavitating flows," Int. J. Multiphase Flow **70**, 22–34 (2015).
[6]P. Huang, G. Coleman, and P. Bradshaw, "Compressible turbulent channel flows: DNS results and modelling," J. Fluid Mech. **305**, 185–218 (1995).
[7]O. Coutier-Delgosha, J. Reboud, and Y. Delannoy, "Numerical simulation of the unsteady behaviour of cavitating flows," Int. J. Numer. Methods Fluids **42**, 527–548 (2003).
[8]J. Decaix and E. Goncalves, "Time-dependent simulation of cavitating flow with k–l turbulence models," Int. J. Numer. Methods Fluids **68**, 1053–1072 (2012).
[9]M. Brunhart, C. Soteriou, M. Gavaises, I. Karathanassis, P. Koukouvinis, S. Jahangir, and C. Poelma, "Investigation of cavitation and vapor shedding mechanisms in a Venturi nozzle," Phys. Fluids **32**, 083306 (2020).
[10]J. Decaix and E. Goncalves, "Compressible effects modeling in turbulent cavitating flows," Eur. J. Mech.-B/Fluids **39**, 11–31 (2013).
[11]J.-L. Reboud, B. Stutz, and O. Coutier, "Two phase flow structure of cavitation: Experiment and modeling of unsteady effects," in 3rd International Symposium on Cavitation CAV1998, Grenoble, France (1998), Vol. 26.
[12]O. Coutier-Delgosha, R. Fortes-Patella, and J.-L. Reboud, "Simulation of unsteady cavitation with a two-equation turbulence model including compressibility effects," J. Turbul. **3**, N58–N65 (2002).

[13]O. Coutier-Delgosha, R. Fortes-Patella, and J.-L. Reboud, "Evaluation of the turbulence model influence on the numerical simulations of unsteady cavitation," J. Fluids Eng. **125**, 38–45 (2003).
[14]L. Zhou and Z. Wang, "Numerical simulation of cavitation around a hydrofoil and evaluation of a RNG κ-ε model," J. Fluids Eng. **130**, 011302 (2008).
[15]O. Coutier-Delgosha, R. Fortes-Patella, J.-L. Reboud, N. Hakimi, and C. Hirsch, "Numerical simulation of cavitating flow in 2D and 3D inducer geometries," Int. J. Numer. Methods Fluids **48**, 135–167 (2005).
[16]L. Tan, B. Zhu, Y. Wang, S. Cao, and S. Gui, "Numerical study on characteristics of unsteady flow in a centrifugal pump volute at partial load condition," Eng. Comput. **32**, 1549 (2015).
[17]O. Coutier-Delgosha, B. Stutz, A. Vabre, and S. Legoupil, "Analysis of cavitating flow structure by experimental and numerical investigations," J. Fluid Mech. **578**, 171–222 (2007).
[18]S. Frikha, O. Coutier-Delgosha, and J. A. Astolfi, "Influence of the cavitation model on the simulation of cloud cavitation on 2D foil section," Int. J. Rotating Mach. **2008**, 1.
[19]B. Charrière, J. Decaix, and E. Goncalvès, "A comparative study of cavitation models in a Venturi flow," Eur. J. Mech.-B/Fluids **49**, 287–297 (2015).
[20]S. Jahangir, E. C. Wagner, R. F. Mudde, and C. Poelma, "Void fraction measurements in partial cavitation regimes by x-ray computed tomography," Int. J. Multiphase Flow **120**, 103085 (2019).
[21]H. Xiao and P. Cinnella, "Quantification of model uncertainty in RANS simulations: A review," Prog. Aerosp. Sci. **108**, 1–31 (2019).
[22]I. Khlifa, A. Vabre, M. Hočevar, K. Fezzaa, S. Fuzier, O. Roussette, and O. Coutier-Delgosha, "Fast X-ray imaging of cavitating flows," Exp. Fluids **58**, 157 (2017).
[23]G. Zhang, I. Khlifa, and O. Coutier-Delgosha, "Experimental investigation of turbulent cavitating flows in a small Venturi nozzle," in *Fluids Engineering Division Summer Meeting* (American Society of Mechanical Engineers, 2019), Vol. 59087, p. V005T05A011.
[24]G. Zhang, I. Khlifa, K. Fezzaa, M. Ge, and O. Coutier-Delgosha, "Experimental investigation of internal two-phase flow structures and dynamics of quasi-stable sheet cavitation by fast synchrotron x-ray imaging," Phys. Fluids **32**, 113310 (2020).
[25]L. Zhang, G. Zhang, M. Ge, and O. Coutier-Delgosha, "Experimental study of pressure and velocity fluctuations induced by cavitation in a small Venturi channel," Energies **13**, 6478 (2020).
[26]F. R. Menter, "Two-equation eddy-viscosity turbulence models for engineering applications," AIAA J. **32**, 1598–1605 (1994).
[27]F. R. Menter, M. Kuntz, and R. Langtry, "Ten years of industrial experience with the SST turbulence model," (Begell House, Inc., Antalya, Turkey, 2003).
[28]B. Ji, X. Luo, R. E. Arndt, and Y. Wu, "Numerical simulation of three dimensional cavitation shedding dynamics with special emphasis on cavitation–vortex interaction," Ocean Eng. **87**, 64–77 (2014).
[29]E. L. Amromin and R. E. Arndt, "Analysis of influence of cavity content on flow pulsations," Int. J. Multiphase Flow **110**, 108–117 (2019).
[30]A. K. Singhal, M. M. Athavale, H. Li, and Y. Jiang, "Mathematical basis and validation of the full cavitation model," J. Fluids Eng. **124**, 617–624 (2002).
[31]E. Goncalves, M. Champagnac, and R. Fortes Patella, "Comparison of numerical solvers for cavitating flows," Int. J. Comput. Fluid Dyn. **24**, 201–216 (2010).
[32]J. Zhu, "A low-diffusive and oscillation-free convection scheme," Commun. Appl. Numer. Methods **7**, 225–232 (1991).
[33]S. Patankar, *Numerical Heat Transfer and Fluid Flow* (CRC Press, 2018).
[34]C. Sarraf, Y. Ait Bouziad, H. Djeridi, M. Farhat, F. Deniset, and J.-Y. Billard, "Effect of cavitation on the structure of the boundary layer in the wake of a partial cavity," in *6th International Symposium on Cavitation CAV2006* (Wageningen, The Netherlands, 2006).
[35]V. Aeschlimann, S. Barre, and H. Djeridi, "Velocity field analysis in an experimental cavitating mixing layer," Phys. Fluids **23**, 055105 (2011).
[36]K. Benoit, "Linear regression models with logarithmic transformations," London School Econ., London **22**, 23–36 (2011).
[37]H. Schlichting, "Boundary layer theory," (McGraw-Hill, New York, 1979).
[38]M. Bhatt and K. Mahesh, "Numerical investigation of partial cavitation regimes over a wedge using large eddy simulation," Int. J. Multiphase Flow **122**, 103155 (2020).
[39]Y. Wang, C. Huang, X. Fang, X. Yu, X. Wu, and T. Du, "Cloud cavitating flow over a submerged axisymmetric projectile and comparison between two-dimensional RANS and three-dimensional large-eddy simulation methods," J. Fluids Eng. **138**, 061102 (2016).
[40]Z.-H. Liu, B.-L. Wang, X.-X. Peng, and D.-C. Liu, "Calculation of tip vortex cavitation flows around three-dimensional hydrofoils and propellers using a nonlinear $k-\varepsilon$ turbulence model," J. Hydrodynamics, Ser. B **28**, 227–237 (2016).
[41]A. Asnaghi, U. Svennberg, and R. E. Bensow, "Large eddy simulations of cavitating tip vortex flows," Ocean Eng. **195**, 106703 (2020).
[42]J. Wu, H. Xiao, R. Sun, and Q. Wang, "Reynolds-averaged Navier–Stokes equations with explicit data-driven Reynolds stress closure can be ill-conditioned," J. Fluid Mech. **869**, 553–586 (2019).
[43]X. Zhang, J. Wu, O. Coutier-Delgosha, and H. Xiao, "Recent progress in augmenting turbulence models with physics-informed machine learning," J. Hydrodynamics **31**, 1153–1158 (2019).
[44]X. Zhang, H. Xiao, T. Gomez, and O. Coutier-Delgosha, "Evaluation of ensemble methods for quantifying uncertainties in steady-state CFD applications with small ensemble sizes," Comput. Fluids **203**, 104530 (2020).
[45]K. Duraisamy, G. Iaccarino, and H. Xiao, "Turbulence modeling in the age of data," Annu. Rev. Fluid Mech. **51**, 357–377 (2019).